Energy 262 (2023) 125289

Contents lists available at ScienceDirect

Energy

journal homepage: www.elsevier.com/locate/energy

The use of a thermal diode bridge for passive temperature control in the built environment during the heating seasons – An analytical study

Yongjia Wu [a], Shifeng Yu [b], Caixia Wang [a,*], Qiong Chen [a], Tingzhen Ming [a,**]

[a] School of Civil Engineering and Architecture, Wuhan University of Technology, No. 122, Luoshi Road, Wuhan 430070, China
[b] School of Electrical Engineering, State Key Laboratory of Power Transmission Equipment & System Security and New Technology, Chongqing University, 174 Shazheng Street, Shapingba District, Chongqing 400044, China

ARTICLE INFO

Keywords:
Built environment
Passive temperature control
Thermal diode
Phase change materials
Solar energy

ABSTRACT

The utilization of solar energy to maintain a stable and comfortable air temperature in the built environment has opened up many opportunities for energy saving. However, the periodical nature of the sunlight intensity introduced extra difficulty in the utilization of solar energy. In this paper, a novel concept of jointly using a thermal diode bridge (TDB) and phase change materials (PCMs) was proposed to continuously control the air temperature in built environments during the heating seasons. During the daytime, the solar energy was efficiently harvested and stored in the PCMs, so the indoor temperature was significantly reduced; at nighttime, the thermal energy stored in the PCMs could be used for space heating without heat loss to the outdoor through heat convection. Because of the existence of the TDB, the heat flux going through the building envelope could be passively controlled. An analytical study to evaluate the operating performance of applying such TDB to controlling the zone air temperature in a built environment was carried out and the results were presented. It was demonstrated that the zone air temperature variation in the built environment was significantly reduced, without any electrical energy consumption and greenhouse gas emission.

1. Introduction

Buildings are designed to shelter occupants and provide them with thermal comfort by using heating ventilation and air conditioning (HVAC) as necessary. Consequently, tremendous energy has been consumed. For example, in 2018, in China, the building sector consumed 22% of the total national energy consumption [1], with a large portion contributed by the HVAC systems. Therefore, a new building design with low energy consumption is critically important in promoting sustainability and carbon neutrality [2]. Developing novel building envelopes with appropriate thermal characteristics [3–5] is an effective way to reduce the building energy consumption.

Conventionally, the energy saving performance of the building envelope is evaluated by the effective heat transfer coefficient. Thermal insulation has been widely used in modern buildings to reduce the effective heat transfer coefficient, thus the space heating and cooling loads in locations with dynamic climatic conditions. The ideal materials for building envelope should have an extremely low thermal conductivity and good constructability at an acceptable price. Insulation materials, such as foamed polyurethane [6], cellulose [7], fiberglass [8], aerogel [9], rock wool [10], polystyrene [11], polyurethane foam [12], and vermiculite [13] are commonly used in the buildings. Huang et al. [9] compared the thermal performances of a super-insulated aerogel with four commonly-used insulation materials. It was claimed that the use of the aerogel helped reduce the annual total building cooling and heating loads, as well as greenhouse gas emissions. Al-Homoud [14] presented the basic principles of thermal insulation and introduced the thermal properties of the most commonly used building insulation materials. Kumar and Suman [15] experimentally studied the impact of thermal insulation on thermal comfort and energy saving performances of the buildings in India. It has been shown that thermal insulation is very effective in reducing building energy consumption. However, as the heat transfer coefficient of the building envelope can't be reduced to zero, the energy loss through the building envelope must be balanced by the clean energy to achieve carbon neutralization.

On the other hand, researchers also looked into designing novel building envelopes that could store and release energy in controlled ways to improve indoor thermal comfort levels using passive control methods [15–20]. Integrating phase change materials (PCMs) with

* Corresponding author.
** Corresponding author.
E-mail addresses: caixia.wang@whut.edu.cn (C. Wang), tzming@whut.edu.cn (T. Ming).

https://doi.org/10.1016/j.energy.2022.125289
Received 16 February 2022; Received in revised form 31 May 2022; Accepted 24 August 2022
Available online 3 September 2022
0360-5442/© 2022 Elsevier Ltd. All rights reserved.

Nomenclatures

Symbols

c_p	Thermal capacity of the air, $J/(kg \bullet K)$
c_{PCMs}	Thermal capacity of the PCMs, $J/(kg \bullet K)$
C_a	Effective solar heat gain area coefficient
C_s	Shading coefficient
F_{walls}	Area of the walls, m^2
$F_{windows}$	Area of the windows, m^2
F_{floor}	Area of the floor, m^2
F_{roof}	Area of the roof, m^2
h_0	Convective heat transfer coefficient of the PCMs surface, $W/(m^2 \cdot K)$
H	Latent heat of the PCMs, J/kg
K_{walls}	Heat transfer coefficient of the walls, $W/(m^2 \cdot K)$
$K_{windows}$	Heat transfer coefficient of the windows, $W/(m^2 \cdot K)$
K_{floor}	Heat transfer coefficient of the floor, $W/(m^2 \cdot K)$
K_{roof}	Heat transfer coefficient of the roof, $W/(m^2 \cdot K)$
m_{PCMs}	Mass of the PCMs, kg
q_{rad}	Solar radiation intensity, W/m^2
$Q_{Forward}$	Forward heat flow, W/m^2
$Q_{Reverse}$	Reverse heat flow, W/m^2
Q_{solar}	Solar heat harvested by the TDB, J
Q'_{solar}	Solar heat gain from the windows, J
Q_{walls}	Heating loss through the walls, J
$Q_{windows}$	Heating loss through the windows, J
Q_{floor}	Heating loss through the floor, J
Q_{PCMs}	Heat exchange between the PCMs and the indoor space, J
$Q_{infiltration}$	Heating loss through the infiltration, J
$Q'_{Envelope}$	Heating loss through the building envelope, J
r	Window to wall ratio
R_{walls}	Thermal resistance of the walls, K/W
$R_{windows}$	Thermal resistance of the windows, K/W
R_{floor}	Thermal resistance of the floor, K/W
R_{roof}	Thermal resistance of the roof, K/W
$R'_{Envelope}$	Thermal resistance of the roof, K/W
t	Time, *hours*
T_s	Temperature of the solar radiation absorption surface, ^oC
T_{PCMs}	Temperature of the PCMs, ^oC
T_{room}	Temperature of the built environment, ^oC
$T_{ambient}$	Outdoor temperature, ^oC
T_{melt}	Average phase change temperature, ^oC
ΔT	Temperature range for melting, ^oC
T_{LCST}	The lower critical solution temperature, ^oC
V	Volume of the room, m^3
φ	Rectification ratio
ρ_{air}	Density of the air, kg/m^2
φ	Solar gain coefficient of the windows
χ	Air tightness
ε	Solar utilization efficiency of the TDB

Abbreviations

HVAC	Heating, ventilation and Air Conditioning
PCMs	Phase change materials
TD	Thermal diode
TDB	Thermal diode bridge

building envelopes such as walls, ceilings, and floors to capture and store solar energy for the zone air temperature control in a built environment has been an essential approach to low energy building design [1,21–26]. Appropriate PCMs for the building application should have suitable melting points, a high thermal capacity, a low thermal expansion coefficient during phase change, and excellent chemical stability. Berardi and Gallardo [21] presented a comprehensive review on incorporating suitable PCMs into concrete. They summarized the impacts of different PCMs and different incorporation methods on the physical, mechanical and thermal properties of incorporated concrete. Recently, Fateh et al. [22] developed a mathematical model to analyze the influence of integrating a layer of PCMs into a typical lightweight wall on its thermal performances. Stritih et al. [23] studied using a composite wall filled with different PCMs to reduce building energy consumption. Li et al. [24] evaluated the energy-saving performance of a novel triple-pane building envelope filled with PCMs. Such a novel envelope could also help reduce indoor air temperature fluctuation. Han and Taylor [25] found out that using PCMs in building envelopes could save up to 17% of the annual HVAC energy consumption. Akeiber et al. [1] reviewed the recent studies of using PCMs for passive building cooling. They suggested that the PCMs to be effectively incorporated into building envelopes should meet several selection criteria. Ahangari and Maerefat [26] introduced an innovative double-layer PCMs design to improve indoor thermal comfort and minimize energy demand in the built environment. Schossig et al. [27] demonstrated a micro-encapsulation method that can easily integrate PCMs into conventional building materials. Ahmad et al. [28] described the thermal performance of light wallboards containing PCMs subjected to climatic variation. Simulation and experimental results demonstrated that the use of building components incorporated PCMs improved the thermal inertia of building envelopes and thus indoor thermal comfort. A comprehensive review on thermal energy storage using PCMs for building applications was given by Khudhair and Farid et al. [29].

Researchers also devoted tremendous efforts to develop technologies to actively control the temperature of the built environment. Li et al. [30] proposed a pipe-embedded wall integrated with ground-source heat exchanger and investigates its energy saving potentials in five typical climate regions of China. They found that the heating load of a house in Beijing was decreased by 18.4%. Shen and Li [31] studied the energy saving performance of a double skin facade with evaporative water circulated inside. The results showed that the cooling strategy was effective and most solar radiation could be taken away. Yan et al. [32,33] developed a new wall system with pipe-encapsulated PCMs and nocturnal sky radiator integrated to reduce the building energy consumption. The cooling loads of the building was reduced by more than 30%.

In recent years, using PCMs to stabilize the air temperature inside a built environment has attracted significant research attention. However, several issues should be addressed before PCMs could be practically applied to real buildings for passively controlling indoor air temperature in both cooling and heating seasons. For example, during the heating seasons, because of the heat transfer between the building envelope and ambient air (the ambient refers to outdoor conditions in this paper), a significant portion of the heat stored in PCMs can be lost into ambient air rather than used for space heating purposes [34]. What's worse, during the cooling seasons, the heat stored in PCMs would even increase the cooling loads [35]. Therefore, how to effectively use the energy stored in the PCMs was not fully explored.

The thermal diode (TD) is a unique thermal component, whose positive and negative heat transfer coefficients differ significantly. During the heating seasons, a TD would allow solar energy to enter an indoor space but cut off its way back to the outdoors. Thus, solar energy could be effectively harvested for space heating. During the cooling seasons, incoming solar energy to an indoor space could be blocked by a TD, so the energy required for space cooling could be significantly reduced. For example, the TD has been used to control the radiative heat

transfer directions for passive radiative cooling [36]. Though radiative cooling reduces the cooling loads in the cooling seasons, it also increases the heating loads in the heating seasons. Tang et al. [36] solved this problem by coating a layer of the tungsten-doped vanadium dioxide on the radiative cooling material that was painted on the window glass or the rooftop. Due to the metal-insulator transition, the transmittance and emissivity of the tungsten-doped vanadium dioxide changed significantly near the transition temperature (around 30 °C) and turned off the radiative cooling at lower temperatures. Wang et al. [37] developed this idea and formulated a scalable thermochromic smart window with passive radiative cooling regulation. Because of the introduction of the unique duel functional TD, the short-wave solar radiation and the long-wave infrared window radiation were controlled simultaneously.

In this paper, a thermal diode bridge (TDB) was constructed by combining a TD with PCMs together. The TDB was able to control the solar gains of the building and stabilize the indoor air temperature for both cooling and heating seasons. The TDB could be integrated into the roof to control the indoor air temperature during the heating seasons purely relying on solar energy. A detailed mathematical model was established to evaluate the operating performances of the TDB for passive indoor air temperature control. This was the first time a TDB was proposed and studied for built environment temperature control. The TDB concept proposed in this paper represented many opportunities for the design of next-generation green buildings with zero energy consumption and carbon emission.

2. The working principles of the TD and the TDB

2.1. The working principle of the TD

Like the electrical diode, the TD is a unique thermal element that can rectify heat flux for specific applications. The characteristic of a typical TD is shown in Fig. 1. At a particular temperature of reference, the magnitudes of thermal energy going through the thermal diode for the positive and negative temperature gradients differ significantly. The performance of the TD is characterized by the rectification ratio [38], which is defined as

$$\varphi = ||Q_{Forward}| - |Q_{Reverse}|| \,/\, |Q_{Reverse}| \quad (1)$$

Due to the nonlinear thermal characteristics of the TD, the forward heat flux is much higher than the reverse one for the same temperature gradient magnitude. The unique function of the TD makes it very useful in the case where a one-way heat transfer is desired.

There are many ways to design a TD. The simplest way to construct a TD is to combine two materials with highly nonlinear temperature-dependent thermal conductivities [39]. In the forward mode, both materials have high thermal conductivities, and the heat flux going through the TD is high. On the contrary, in the reverse mode, the thermal conductivities of both materials change to a small value, and the heat flux is dramatically reduced. For example, the PCMs are often used to construct the TDs because their thermal conductivities vary significantly during the phase transition. Other TDs with large rectification ratios include the fluid loop type [39], thermal expansion type [40], thermal radiation type [41], gravity heat pipe, and hybrid type [42]. The rectification ratios of some TDs were reported larger than 16 in the recent literature [41,43], or even larger than 100 for some specific designs [42]. The high-performance TD design is still an active research area. The future applications of the TD in building temperature control represent a lot of opportunities for energy saving.

2.2. The working principle of the TDB for building application

A passive TDB designed for the built environment temperature control is demonstrated in Fig. 2. There are five critical layers in the TDB, including the glass, thermochromic hydrogel, transparent aerogel thermal isolation, solar radiation absorption surface, and PCMs. The function of each layer is described as follows: (1) The glass layer works as a protection layer. (2) The thermochromic hydrogel can change the light transparency according to the ambient temperature. The lower critical solution temperature (LCST) of PNIPAm hydrogel is about 25 °C. Zhou et al. [44,45] reported that the 200 μm PNIPAm hydrogel thin film was observed to change from transparent at 25 °C to opaque above 35 °C. The thermochromic hydrogel works as a solar radiation switcher in the TDB design. It allows the solar radiation enters the indoor space when the ambient temperature is lower than T_{LCST}, while blocking the solar radiation for a high ambient temperature [37]. (3) The aerogel with ultralow thermal conductivity and greenhouse selectivity is used to cover the solar radiation absorption surface, reducing the thermal energy loss through conduction, convection, and radiation. According to a recent paper published by Zhao et al. [46], a solar receiver covered with ultra-low thermal-conductivity aerogel could harvest more than 80% of the solar radiation energy, creating a temperature higher than 200 °C. (4) The solar radiation absorption surface works as a receiver to harvest solar radiation energy efficiently. (5) The PCMs, working as a heat reservoir, are connected to the back of the solar radiation absorption surface.

In the heating situation ($T_{ambient} \leq T_{LCST}$), the thermochromic

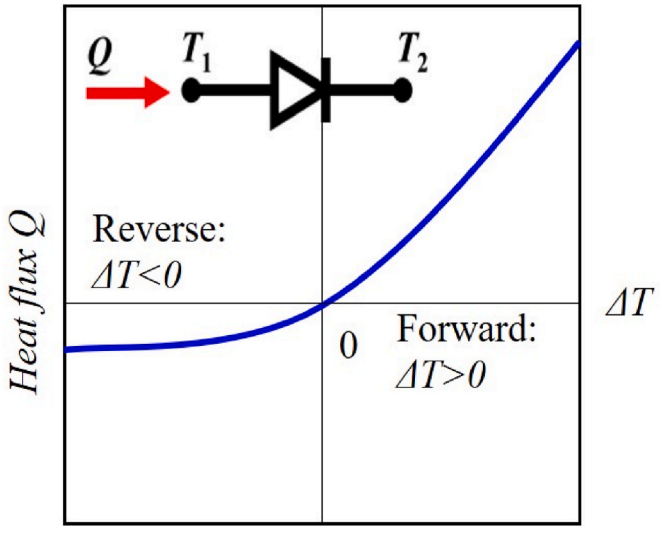

Fig. 1. The working principle of the TD.

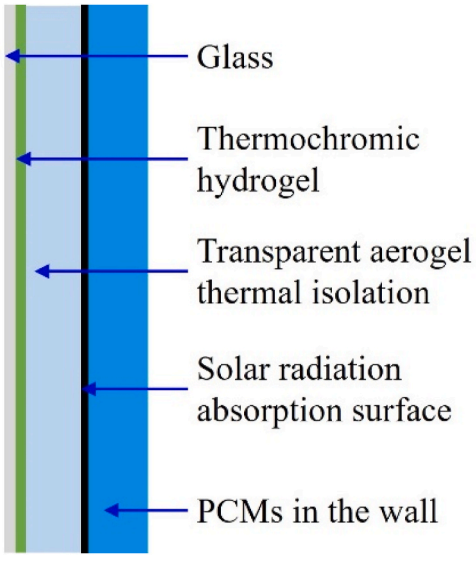

Fig. 2. A TDB integrated into the building envelope for energy savings.

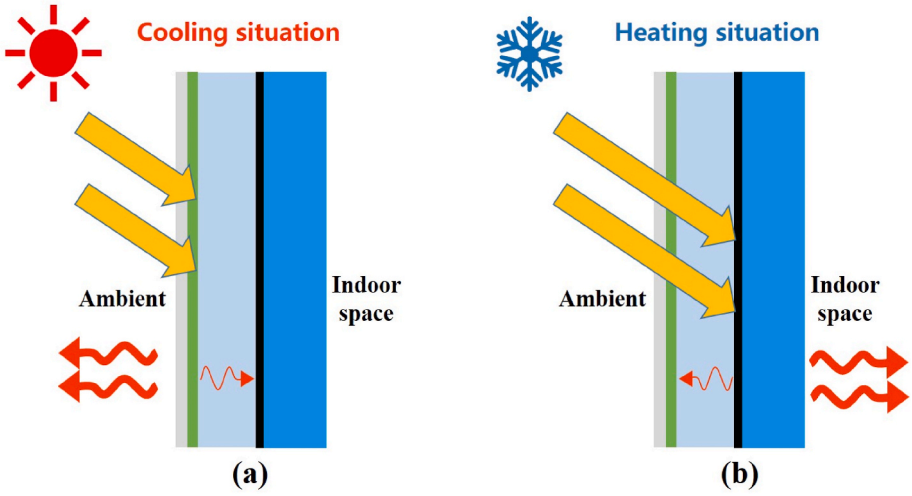

Fig. 3. TDB designed for the passive temperature control of the built environment: (a) cooling situation; (b) heating situation.

hydrogel is transparent, the solar radiation penetrates the transparent thermal isolation layer and is absorbed by the solar radiation absorption surface at the daytime. Because of the transparent aerogel with ultra-low thermal conductivity, the heat absorbed by the solar receiver cannot escape to the ambient but is effectively stored in the PCMs. Thus, the solar energy stored in the PCMs can be efficiently used to heat the indoor space. In the cooling situation ($T_{ambient} > T_{LCST}$), the thermochromic hydrogel became opaque, most of the solar radiation is reflected or absorbed by the thermochromic hydrogel. The solar heat deposited on thermochromic hydrogel can hardly be transported to the indoor space due to the aerogel thermal isolation with ultralow thermal conductivity and greenhouse selectivity. In this way, the TDB can effectively use solar energy for heating purposes during the heating situation, while reducing the cooling loads during the cooling situation. The passive TDB can change its thermal characteristics according to the ambient temperature, which shows its potential applications across the different climate zones. In this paper, the TDB is integrated into the roof of a house, and its influence on the temperature of the built environment during the heating seasons is analyzed by a mathematical model systematically (see Fig. 3).

3. Mathematical model

3.1. Heat transfer model of the TDB during the heating seasons

A mathematical model is established to study the influence of the TDB on the temperature of the built environment during the heating seasons. Because the time scales for the heat transfer process in the built environment and PCMs are much smaller than that for the temperature variation in the ambient, the temperatures of the built environment and PCMs are assumed to be uniform. The energy demand for ventilation isn't considered in the model because highly effective energy recycling technologies can significantly reduce energy loss for low-energy buildings [47,48]. The thermal networks of the TDB during the heating seasons, including the daytime mode the night mode, are given by Fig. 4.

During the heating seasons, as the ambient temperature is lower than LCST of the thermochromic hydrogel, the thermochromic hydrogel became transparent for the solar radiation. Thus, the solar energy harvested by the TDB is given by

$$Q_{solar} = F_{roof}\varepsilon q_{rad} \tag{2}$$

The solar radiation energy is stored in the PCMs continuously during the daytime. The thermal mass of the PCMs should be large enough to hold the energy received.

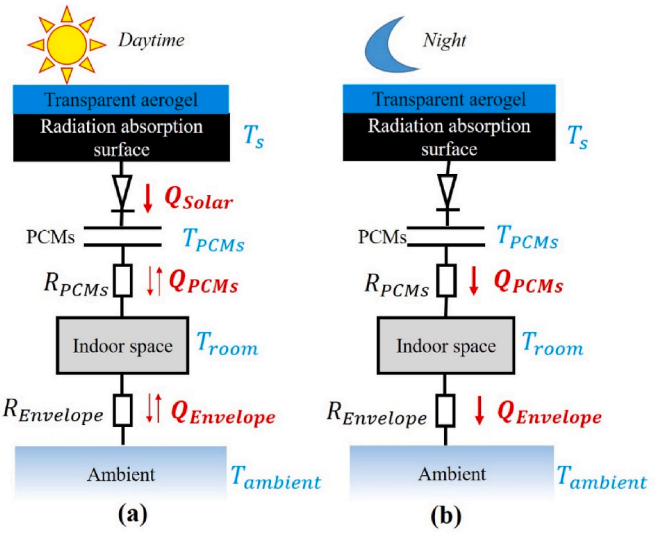

Fig. 4. The thermal network of the TDB during the heating seasons: (a) daytime mode; (b) night mode.

$$m_{PCMs} = \int_{daily} Q_{solar}dt/H \tag{3}$$

where the H is the latent heat of the PCMs. For most commercial PCMs products [1,49], the latent heat ranges from 50 to 250 kJ/kg. The PCMs mass required for the solar energy storage varies from 500 to 100 kg for the house as built in this paper. The thickness of the PCMs layer in the TDB is less than 5 mm, thus the temperature of the PCMs is assumed to be uniform. Usually, the PCMs start to melt at a specific temperature, and melt completely with a small temperature increase of ΔT. In addition, the mass fraction of the liquid increases with the temperature in this narrow temperature window. For simplification, the temperature of the PCMs is assumed to be a constant during the melting process in this paper.

Case One: Solar energy meets the heating demand.

If the energy harvested by the TDB is larger than that required for the heating purpose, the net heat gain of the building should be larger than zero under the design condition. Appointing the heat transfer direction from the ambient to the room as positive, the net heat gain of the building is given by

$$\int_{daily}\left(Q_{solar}+Q'_{solar}+Q_{walls}+Q_{windows}+Q_{floor}+Q_{infiltration}\right)dt\geq 0 \tag{4}$$

where Q_{solar} and Q'_{solar} are the solar heat gains from the TDB and windows, respectively, Q_{walls}, $Q_{windows}$, Q_{floor}, and $Q_{infiltration}$ are the heat loss through walls, windows, floor, and cold air infiltration, respectively.

In this case, the PCMs will not fully be melted or solidified. Thus, the temperature of the PCMs will stay constant.

$$T_{PCMs}=T_{melt} \tag{5}$$

The solar energy harvested by the TDB and the solar heat gains from the windows are dissipated to the ambient through the building envelope and cold air infiltration. An energy balance is established for the built environment.

$$Q_{walls}+Q_{windows}+Q_{floor}+Q_{PCMs}+Q_{infiltration}+Q'_{solar}=V\rho_{air}c_p\frac{dT_{room}}{dt} \tag{6}$$

The thermal resistances of the walls and windows are given by Eqs. (7) and (8).

$$R_{walls}=\frac{1}{K_{walls}F_{walls}} \tag{7}$$

$$R_{windows}=\frac{1}{K_{windows}F_{windows}} \tag{8}$$

Generally, the heat loss through the floor is calculated based on the assumption that the temperature is a constant at some space below the ground. In this paper, the heat loss through the floor is calculated by connecting the floor to ambient as the temperatures under the ground vary in different regions around the world. Usually, the floor near the walls contributes more heat loss. Thus, the floor is divided into five zones for heat transfer analysis, as shown in Fig. 5.

$$R_{floor}=\frac{1}{\sum_1^5 K_{floor\_i}F_{floor\_i}} \tag{9}$$

In this model, the TDB is integrated into the roof of the house. The convective heat transfer resistance of the PCMs surfaces is

$$R_{PCMs}=\frac{1}{h_0F_{roof}} \tag{10}$$

The heat loss to the ambient through the walls, windows, and the floor is calculated by Eqs. (11)–(13), respectively.

$$Q_{walls}=\frac{T_{ambient}-T_{room}}{R_{walls}} \tag{11}$$

$$Q_{windows}=\frac{T_{ambient}-T_{room}}{R_{windows}} \tag{12}$$

$$Q_{floor}=\frac{T_{ambient}-T_{room}}{R_{floor}} \tag{13}$$

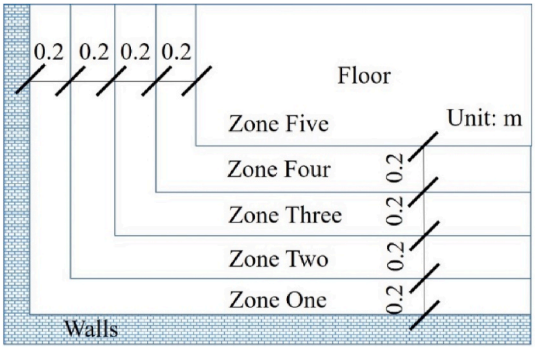

Fig. 5. The heat transfer zones of the floor.

The heat exchange between the PCMs and the built environment is given by Eq. (14).

$$Q_{PCMs}=\left(T_{PCMs}-T_{room}\right)/R_{roof} \tag{14}$$

The solar heat gains from windows can be calculated by Eq. (15).

$$Q'_{Solar}=C_aC_s\varphi F_{windows}q_{rad} \tag{15}$$

Heat loss through cold air infiltration can be given by

$$Q_{infiltration}=\chi V\rho_{air}c_p\left(T_{ambient}-T_{room}\right) \tag{16}$$

Substituting Eqs. (7)–(16) into Eq. (6), the temperature of the built environment can be solved numerically by the improved Euler method, which owns a second-order accuracy.

Case Two: Solar energy cannot meet the heating demand.

If the energy harvested by the TDB is less than that required for the heating purpose, the temperature of the PCMs will vary with the ambient temperature after the solar heat is depleted. The PCMs experienced several statuses during the day.

Stage One: Pre-heating ($T_{PCMs}<T_{Melt}$)

In this stage, the temperature of the PCMs doesn't reach the melting point. The temperature of the PCMs will increase with the absorption of solar energy. An energy balance is built for the PCMs.

$$Q_{Solar}-Q_{PCMs}=m_{PCMs}c_{PCMs}\frac{dT_{PCMs}}{dt} \tag{17}$$

Stage Two: Partially melted ($T_{PCMs}=T_{Melt}$)

In this stage, the PCMs receive the solar energy from the solar absorption surface. The PCMs are partially melted, thus the temperature of the PCMs stays constant.

Stage Three: Pre-solidified ($T_{PCMs}=T_{Melt}$)

In this stage, the solar heat stored in the PCMs is released to the indoor space for heating purposes. Because the PCMs are not fully solidified, the temperature of the PCMs keeps constant.

Stage Four: Fully Solidified ($T\geq T_{Melt}$)

In this stage, the PCMs are solidified. The temperature of the PCMs varies with ambient temperature.

$$Q_{PCMs}=-m_{PCM}c_{PCMs}\frac{dT_{PCMs}}{dt} \tag{18}$$

In this case, the temperatures of the built environment and the PCMs should be solved simultaneously.

3.1.1. Heat transfer model of a regular building envelope

For a regular building envelope, the built environment exchanges heat with the ambient through the building envelope, as shown in Fig. 6. The energy conservation equation for this system is

$$Q'_{envelope}+Q'_{solar}+Q_{infiltration}=V\rho_{air}c_p\frac{dT_{room}}{dt} \tag{19}$$

$$R'_{Envelope}=\frac{1}{K_{walls}F_{walls}+K_{windows}F_{windows}+K_{roof}F_{roof}+\sum_1^5 K_{floor\_i}F_{floor\_i}} \tag{20}$$

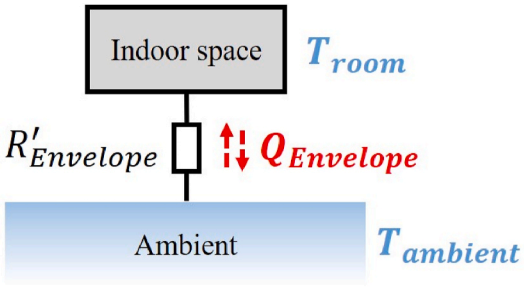

Fig. 6. Thermal network in a regular building envelope. For the regular house, the thermal resistance of the building envelope is given by.

The heat loss through the building envelope can be calculated by Eq. (21).

$$Q'_{envelope} = \frac{T_{ambient} - T_{room}}{R'_{Envelope}} \quad (21)$$

Substituting Eqs. (15), (16) and (21) into Eq. (19), the temperature of the built environment can be obtained by solving Eq. (19) numerically.

3.2. Parameters used for the model

3.2.1. Building model

In this paper, a simplified house is used as an example for the analysis. The house is a one-story building facing due south as shown in Fig. 7. The building is 12.0 m long, 10.0 m wide, and 3.5 m high, with a shape coefficient of 0.65. The window-to-wall ratio of the building envelope is 0.2. According to the thermal characteristics of TDB, as well as relevant design standards currently implemented in China, the heat transfer coefficient, air-tightness, and solar heat gain coefficient of the building envelope structure are listed in Table 1. The convective heat transfer coefficient of the TDB roof on the indoor surface is set as 2.5 W/(m^2·K) [50]. Because the thermal conductivity of the aerogel is extremely low (about 0.02–0.03 W/(m·K)) and the infrared radiation is blocked by the greenhouse-selectivity aerogel, $Q_{reverse}$ of the roof is very small. Meanwhile, the thermal conductivity of the PCMs is in the order of 1.0 W/(m·K) [29]. The rectification ratio of the TDB is about 30–50. For simplification, $Q_{reverse}$ was considered as a part of solar heat loss, which was reflected in the solar heat collection efficiency of the aerogel thermal isolation layer. Bio PCM ENRG blanket made by Phase Change Energy Solutions is adopted as the PCMs for the TDB [49]. The thermal properties of the PCMs are presented in Table 1.

3.2.2. Meteorological data

The meteorological data of four cities in China, including Wuhan, Beijing, Harbin, and Lhasa on January 21, a typical heating day, is used as the input for the modeling. The original meteorological data, including the ambient dry-bulk temperature and solar radiation intensity, is cited from the official website of the China Meteorological Bureau, Climate Data Office. As seen in Fig. 8, the temperature and solar radiation intensity variations of the five cities can be very different. The average temperatures of Wuhan, Beijing, Harbin, and Lhasa are 6.41 °C, −4.37 °C, −20.82 °C, and 1.25 °C, respectively. And the total daily solar radiations of Wuhan, Beijing, Harbin, and Lhasa are 4784 kJ/m^2, 10789.2 kJ/m^2, 7196.4 kJ/m^2, and 17827.2 kJ/m^2, respectively.

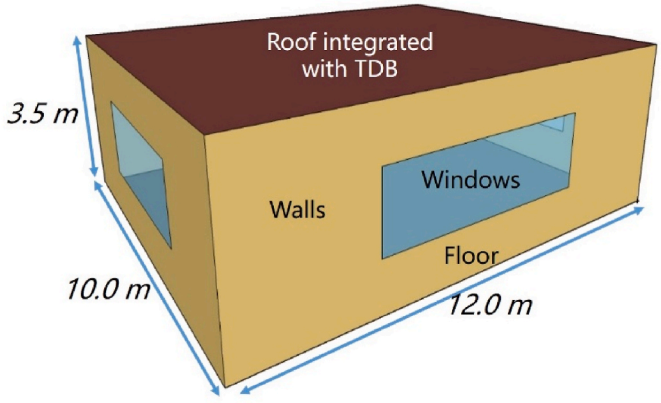

Fig. 7. The building model for the analysis.

Table 1
Design parameters of the building envelope.

Parameters		House with traditional roof	House with TDB roof
Window-to-wall ratio (in all directions)		0.2	0.2
Heat transfer coefficient of the exterior walls (W/(m^2·K))		0.517[a]	0.517
Heat transfer coefficient of the exterior windows (W/(m^2·K))		1.9[b]	1.9
Heat transfer coefficient of the roof (W/(m^2·K))		0.45[c]	N/A
Heat transfer coefficients of the floor (W/(m^2·K))	Zone One	0.46[d]	0.46
	Zone Two	0.23	0.23
	Zone Three	0.12	0.12
	Zone Four	0.07	0.07
	Zone Five	Neglected	Neglected
Effective solar heat gain area coefficient of the windows		0.25	0.25
Shading coefficient of the windows		0.8	0.8
Solar heat gain coefficient of the windows		0.4	0.4
Convective heat transfer coefficient of the TDB roof on the indoor surface (W/(m^2·K))		N/A	2.5 [50]
Solar utilization efficiency of the TDB		N/A	0.20–0.60[e] [37,46]
Phase change temperature of the PCMs (°C)		N/A	17, 20, 23, and 26, respectively
Mass of the PCMs (kg)		N/A	100
Latent heat of the PCMs (kJ/kg)		N/A	200 [49]
Thermal capacity of the PCMs (J/(kg•K))		N/A	2100 [49]
Air density (kg/m^3)		1.225	1.225
Air thermal capacity (J/(kg•K))		1004	1004
Air tightness (Times/hour)		0.28	0.28

[a] The regular energy-saving walls consist the stucco, concrete, wall insulation, and gypsum layers from outside to inside. The thickness of the wall is 0.2863 m.
[b] The windows are constructed by the low-E double-layer insulating glass with an air gap of 12.0 mm.
[c] The regular energy-saving roof consists of the roof membrane, roof insulation, metal decking layers. The thickness of the roof is 0.2215 m.
[d] According to the Design Standard for Energy Efficiency of Civil Buildings in China, the U value for the floor with thermal isolation should be lower than 0.5 W/(m^2·K). In addition, the thermal resistances for the different floor zones are assumed connected in parallel. The heat transfer between different floor zones are neglected.
[e] Solar utilization efficiency of the TDB is affected by the solar radiation transmittance of the thermochromic hydrogel and the solar heat collection efficiency of the aerogel thermal isolation layer. The solar heat collection efficiency of the aerogel thermal isolation layer changes between 70% and 90% depending on the thickness [46]. And the spectral solar radiation transmittance of the thermochromic hydrogel varied from 30% to 90% [37]. Thus, the solar utilization efficiency of TDB can vary from 0.2 to 0.6.

4. Results and discussion

4.1. The temperature control performance of the TDB

The temperature of the built environment is affected by the ambient via heat exchange through the building envelope. The zone air temperature variations for the building envelope integrated with/without the TDB are shown in Fig. 9. For the regular building envelope, the temperature of the built environment fluctuates with the ambient temperature and solar radiation intensity. The average temperatures of the built environment for the regular building are slightly higher than the average temperature of the ambient for all four cities. Because of the solar heat gain from the windows during the daytime, the temperature of the built environment is significantly higher than the ambient around

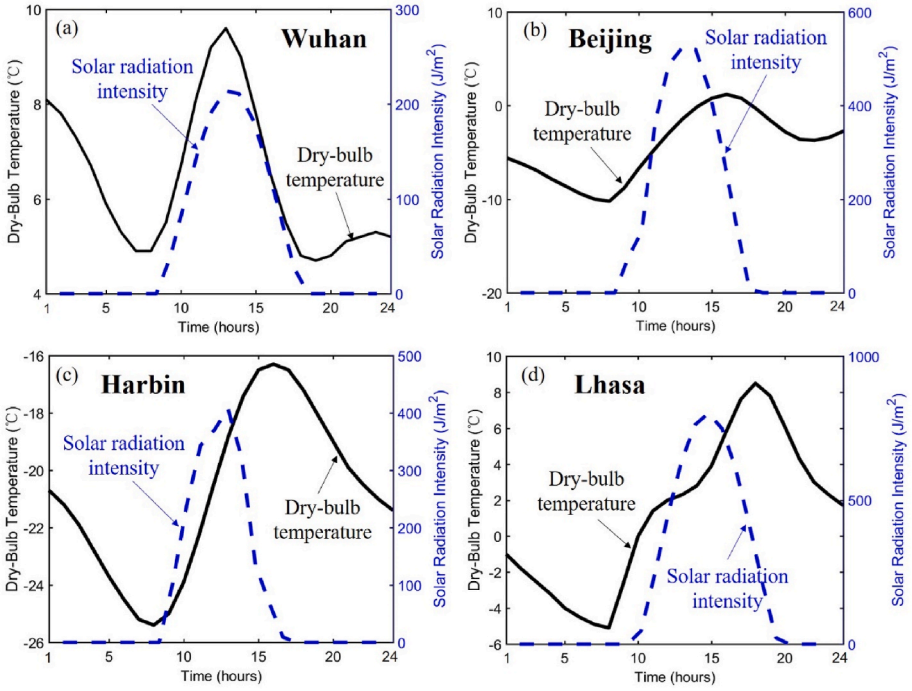

Fig. 8. Meteorological data of (a) Wuhan; (b) Beijing; (c) Harbin; (d) Lhasa on January 21 in a typical meteorological year.

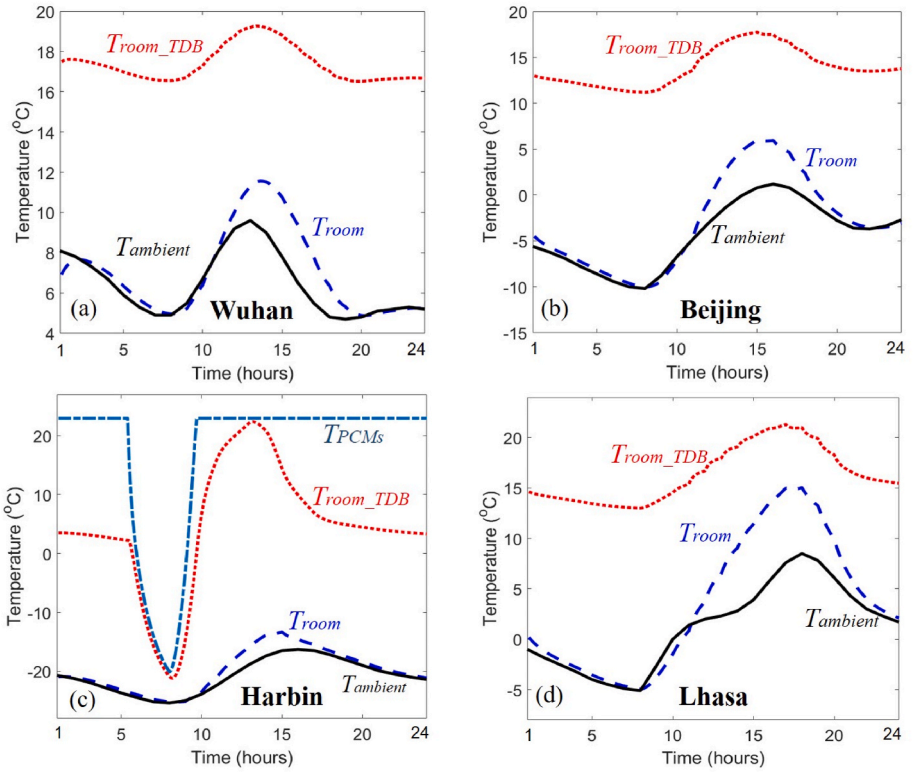

Fig. 9. The zone air temperature variations: (a) Wuhan; (b) Beijing; (c) Harbin; and (d) Lhasa when $T_{melt} = 23.0\ ^{\circ}C$, $\varepsilon = 0.4$.

1:00 p.m. when the solar radiation is highest during the day.

Due to the novel TDB, solar energy can be effectively harvested for the passive temperature control of the built environment. The average zone air temperatures of house integrated with TDB in Wuhan, Beijing, Harbin, and Lhasa are 17.92 °*C*, 14.85 °*C*, 3.50 °*C*, and 16.18 °*C*, respectively, which are increased by 11.49 °*C*, 19.22 °*C*, 24.32 °*C*, and 14.93 °*C*, respectively. It is impressive to see that the building integrated with the TDB can increase the zone air temperature to such a large extent that the houses in Wuhan, Beijing, and Lhasa can almost maintain a stable and comfortable temperature during the whole day without any external energy supply. However, because the ambient temperature in Harbin is very low in the winter, the solar energy harvested by the TDB

can't meet the energy demand for heating purposes. As shown in Fig. 9 (c), the solar energy stored in the PCMs is depleted around 5:00 a.m., and the zone air temperature drops quickly to the ambient temperature. Though the TDB alone can't achieve the goal to create a comfortable built environment in Harbin, it helps to increase the average zone air temperature greatly and in turn reduce the heating demands.

4.2. The influence of phase change temperature of the PCMs

Fig. 10 shows the zone air temperature variations of the house in Harbin with all the parameters set the same except the phase change temperature of the PCMs. When $T_{melt} = 17\ ^{\circ}C$, the temperature of the PCMs can marginally keep stable during the day. However, with T_{melt} changing from 17 °C to 26 °C, the temperature of the PCMs fluctuates dramatically late at night. Because the temperature difference between the PCMs and the built environment is larger for the PCMs with a higher T_{melt}, the heat stored in the PCMs with a higher T_{melt} depletes more quickly. As shown in Fig. 10, the period that the PCMs loses function enlarged quickly with a higher T_{melt}. And the lowest zone air temperatures happen around 8:00 a.m., which are −1.79 °C, −15.23 °C, −21.18 °C, and −23.42 °C for $T_{melt} = 17\ ^{\circ}C$, 20 °C, 23 °C, and 26 °C, respectively. The average zone air temperatures are 4.01 °C, 4.35 °C, 4.43 °C, and 4.41 °C for $T_{melt} = 17\ ^{\circ}C$, 20 °C, 23 °C, and 26 °C, respectively. It can be seen that the phase change temperature of the PCMs has a very small influence on the average zone air temperature. However, the zone air temperature fluctuates amplitude varies dramatically with the phase change temperature of the PCMs during the day. It is also observed that the phase change temperature of the PCMs is not always higher than the zone air temperature, because the windows solar heat gain can also help to increase the zone air temperature.

The influence of the phase change temperature on the zone air temperature is very different for the house in other three cities. Taking Beijing for example, because the solar radiation in Beijing is much higher than in Harbin, the ambient temperature is also warmer. The TDB can always meet the energy demand for heating purposes. As shown in Fig. 11, the average zone air temperatures are 10.04 °C, 11.99 °C, 13.92 °C, and 15.85 °C for $T_{melt} = 17\ ^{\circ}C$, 20 °C, 23 °C, and 26 °C, respectively. The zone air temperature almost increases linearly with T_{melt}. And the zone air temperature fluctuation amplitude is almost the same for all the cases.

The appropriate phase change temperatures of the PCMs for the buildings in different climate regions are different. For the regions where solar energy is abundant, a relatively higher phase change temperature of the PCMs will help to increase the average temperature of

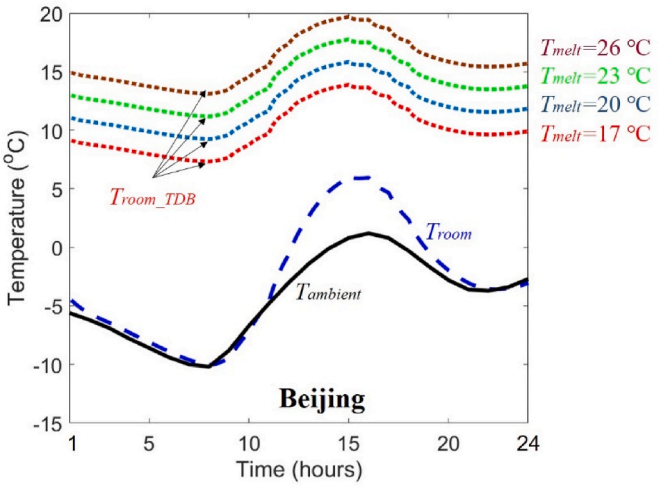

Fig. 11. Zone air temperature variations of the house in Beijing with T_{melt} ranging from 17 °C to 26 °C, and $\varepsilon = 0.4$.

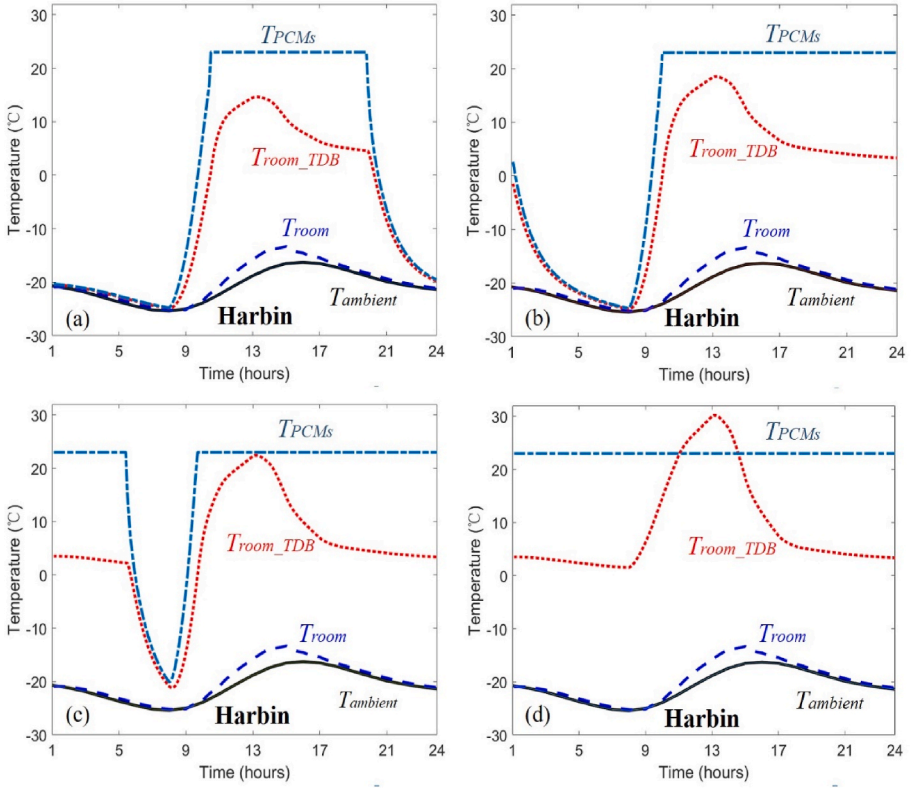

Fig. 10. Zone air temperature variations of the house in Harbin with (a) $T_{melt} = 17\ ^{\circ}C$, $\varepsilon = 0.4$; (b) $T_{melt} = 20\ ^{\circ}C$, $\varepsilon = 0.4$; (c) $T_{melt} = 23\ ^{\circ}C$, $\varepsilon = 0.4$; (d) $T_{melt} = 26\ ^{\circ}C$, $\varepsilon = 0.4$.

the built environment. However, in regions where solar energy alone can't meet the energy demand for heating purposes, the phase change temperature of the PCMs should be relatively lower to maintain a relatively stable temperature in the built environment.

4.3. The influence of the solar utilization efficiency of the TDB

The solar utilization efficiency of the TDB will significantly affect the temperature of the built environment. As shown in Fig. 12, the average zone air temperatures of the house in Harbin are −7.58 °C, −1.47 °C, 4.41 °C, and 10.67 °C for $\varepsilon = 0.2$, 0.3, 0.4, and 0.6, respectively. The average zone air temperature increases dramatically with the higher solar utilization efficiency. When $\varepsilon = 0.2$, the PCMs almost lose the function to control the zone air temperature at night. With the $\varepsilon = 0.6$, the temperature of the PCMs can maintain stable during the whole day. Furthermore, the lowest temperature of the built environment rises up to 3.10 °C, 28.1 °C higher than the lowest ambient temperature. With a further increase in the solar utilization efficiency, the zone air temperature doesn't increase anymore. It should be noted that the zone air temperature is higher than the PCMs' temperature because of the windows solar heat gain around noon.

The solar utilization efficiency of the TDB is critically important to effectively control the temperature of the built environment, particularly for the house in the severe cold regions where heating loads are high and solar radiation intensities are small. To enhance the solar utilization efficiency of the TDB, the one-way heat transfer performance of the TDB should be furtherly improved. The transparent aerogel with ultra-low thermal-conductivity and greenhouse selectivity can reduce the heat loss of the TDB by cutting off the ways for heat conduction, convection, and infrared radiation. Zhao et al. [46] reported a solar receiver covered by this material harvested more than 80% of the solar radiation energy, which showed the promising potential of designing such a TDB for passive temperature control in the built environment during the heating seasons.

4.4. Energy saving performance of the TDB

The daily heating loads of the regular buildings in Wuhan, Beijing, and Lhasa are 170.6 MJ, 360.9 MJ, and 236.7 MJ, respectively. The solar energy harvested by the TDB can meet the heating demands of the houses in the three cities without any external energy consumption. The transient heating loads of the house in Harbin with/without TDB are compared in Fig. 13(a), where the goal zone air temperature is set as 16.0 °C. The daily heating loads of the regular building and the building integrated with TDB are 682.7 MJ and 466.3 MJ, respectively. The TDB represents an energy saving rate of 31.7%. As shown in Fig. 13(a), the transient heating loads of the house integrated with TDB are lower than the regular house for most time of the day. However, in the early morning, the heating loads of the house integrated with TDB increases rapidly and exceeds the heating loads of the regular house. Because the solar energy stored in the building environment is depleted at that time period, more energy is required to keep the PCMs and built environment warm.

The heat loss proportions through the building envelope with/without TDB are depicted in Fig. 13(b and c). For the regular building envelope, the heat losses through the floor, infiltration, walls, windows, and roof account for 1.72%, 18.25%, 28.93%, 26.58%, and 24.53%, respectively, of the total heat loss. For the building envelope integrated with TDB, the heat losses through the floor, infiltration, walls, and windows account for 2.28%, 24.18%, 38.33%, and 35.22%, respectively, of the total heat loss. The heat loss through the roof is reduced to a minimum level for the building integrated with TDB, and the energy flows are significantly different from those of the regular building.

5. Conclusions and future efforts

The building sector accounts for a large proportion of the energy consumption among all the energy-end use sectors. The construction of the next-generation green buildings characterized as low energy consumption and low emission requires advanced thermal designs. In this

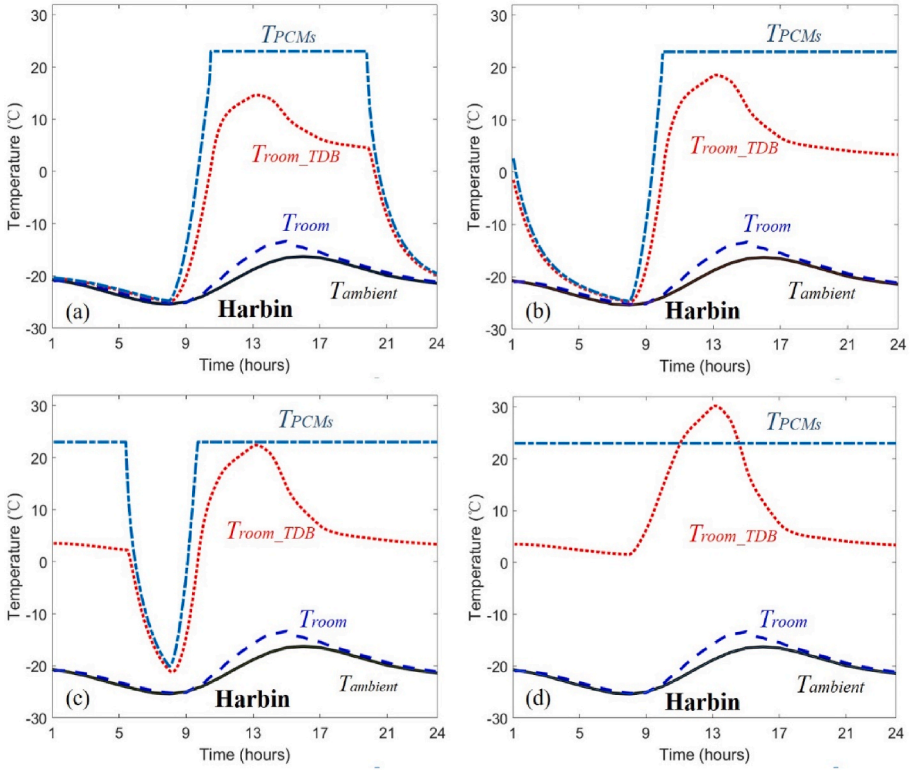

Fig. 12. Zone air temperature variations in the built environment with different solar utilization efficiency: (a) ε = 0.2; (b) ε = 0.3; (c) ε = 0.4; (d) ε = 0.6.

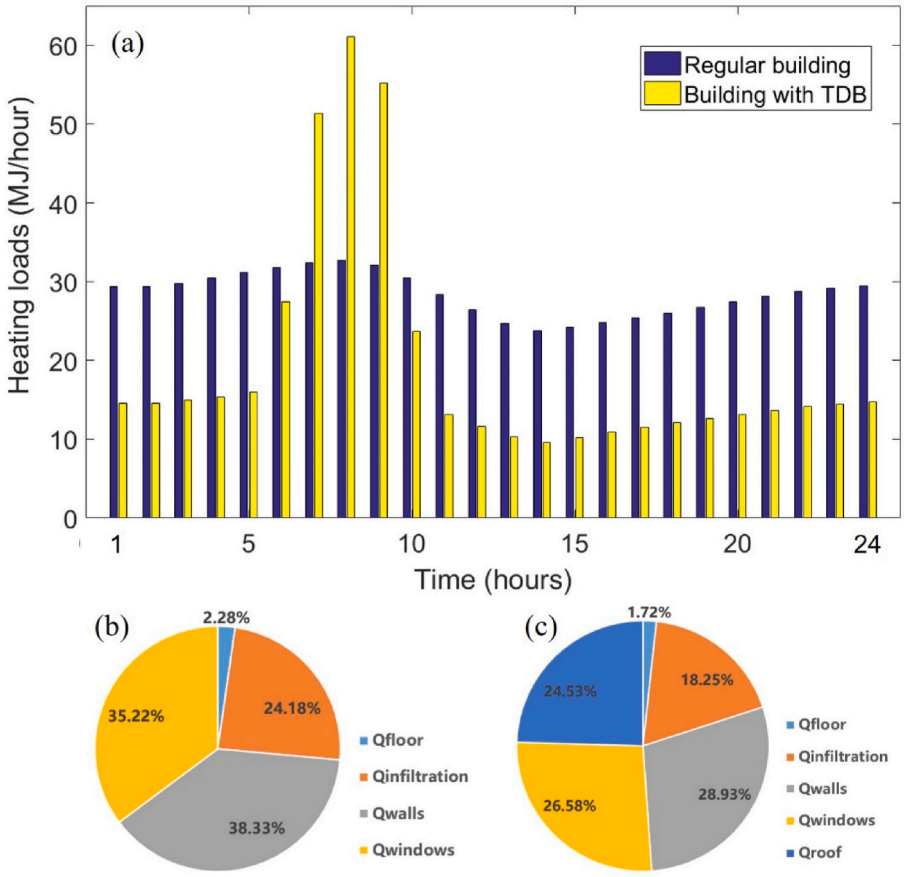

Fig. 13. The comparison of the house heating loads with/without TDB: (a) The transient heat loads of the house in Harbin with/without TDB when $T_{melt} = 23\,^{\circ}C$, $\varepsilon = 0.4$; (b–c) heat loss proportions through the building envelope with/without TDB.

paper, a TDB is proposed and designed to harvest solar energy for passive temperature control in the built environment during the heating seasons. A comprehensive mathematical model is established to analyze the temperature-control performance of the TDB. It can be concluded that:

1) TDB can significantly increase the average zone air temperature and reduce the temperature fluctuation amplitude in the built environment during the heating seasons without any external energy consumption.
2) For different climatic conditions, the phase change temperature of the PCMs should be carefully selected to let the TDB work normally. A higher phase change temperature is desired for regions with higher ambient temperature and abundant solar radiation. A lower phase change temperature is better for regions with the opposite situation.
3) When the solar utilization efficiency of the TDB is too low, the TDB can lose functions during the late-night as the energy harvested by the TDB can't meet the demand for heating purposes. To ensure the normal operation of TDB, particularly for houses in severe cold regions, it is critical to improving the one-way heat transfer performance of the TDB.
4) The solar energy harvested by the TDB alone can meet the energy demand for house heating purposes in Wuhan, Beijing, and Lhasa during the heating seasons for the design conditions. In Harbin, a city located in severe cold region, the TDB saves 31.7% of the energy for heating purposes.

The introduction of the TDB in the next-generation building represents tremendous energy saving, which in turn promotes building a low-carbon and green community. To validate these analytical results, a TDB has been constructed in the lab and experiments are doing to examine the passive temperature control performance of the TDB in the built environment. In addition, the energy saving performance of the TDB during the cooling seasons will be analyzed. The results will be reported in future studies.

Credit author statement

Yongjia Wu: Conceptualization, Methodology, Writing-Original draft preparation, Project administration.; Shifeng Yu: Data Curation, Writing-Reviewing and Editing.; Caixia Wang: Software, Validation.; Qiong Chen: Visualization, Formal analysis.; Tingzhen Ming: Supervision, Funding acquisition.

Declaration of competing interest

The authors declare that they have no known competing financial interests or personal relationships that could have appeared to influence the work reported in this paper.

Acknowledgments

This research was supported by the National Natural Science Foundation of China (Grant No. 51778511), Hubei Provincial Key Research and Design Project (Grant No. 2020BAB129), Scientific Reuter Foundation of Wuhan University of Technology (Grant No. 40120551) and the Fundamental Research Funds for the Central Universities (Grant No. WUT: 2021IVA037 and WUT: 2022IVA031).

References

[1] University BecrcoT. Annual development report of China's building energy saving in 2020. 2020.
[2] Alyami SH, Rezgui Y. Sustainable building assessment tool development approach. Sustain Cities Soc 2012;5:52–62.
[3] Ye L, Cheng ZJ, Wang QQ, Lin HY, Lin CQ, Liu B. Developments of green building standards in China. Renew Energy 2015;73:115–22.
[4] China MOCP. Evaluation standard for green building. 2006.
[5] Li YA, Yang L, He BJ, Zhao DD. Green building in China: needs great promotion. Sustain Cities Soc 2014;11:1–6.
[6] Verdolotti L, Oliviero M, Lavorgna M, Santillo C, Tallia F, Iannace S, et al. Aerogel-like" polysiloxane-polyurethane hybrid foams with enhanced mechanical and thermal-insulating properties. Compos Sci Technol 2021:108917.
[7] Gupta P, Singh B, Agrawal AK, Maji PK. Low density and high strength nanofibrillated cellulose aerogel for thermal insulation application. Mater Des 2018;158:224–36.
[8] An L, Wang J, Petit D, Armstrong JN, Li C, Hu Y, et al. A scalable crosslinked fiberglass-aerogel thermal insulation composite. Appl Mater Today 2020;21:100843.
[9] Huang H, Zhou Y, Huang R, Wu H, Sun Y, Huang G, et al. Optimum insulation thicknesses and energy conservation of building thermal insulation materials in Chinese zone of humid subtropical climate. Sustain Cities Soc 2020;52:101840.
[10] Siligardi C, Miselli P, Francia E, Gualtieri ML. Temperature-induced microstructural changes of fiber-reinforced silica aerogel (FRAB) and rock wool thermal insulation materials: a comparative study. Energy Build 2017;138:80–7.
[11] Cai S, Zhang B, Cremaschi L. Review of moisture behavior and thermal performance of polystyrene insulation in building applications. Build Environ 2017;123:50–65.
[12] Shao H, Zhang Q, Liu H, Guo W, Jiang Y, Chen L, et al. Renewable natural resources reinforced polyurethane foam for use of lightweight thermal insulation. Mater Res Express 2020;7(5):055302.
[13] Li T-T, Chuang Y-C, Huang C-H, Lou C-W, Lin J-H. Applying vermiculite and perlite fillers to sound-absorbing/thermal-insulating resilient PU foam composites. Fibers Polym 2015;16(3):691–8.
[14] Al-Homoud MS. Performance characteristics and practical applications of common building thermal insulation materials. Build Environ 2005;40(3):353–66.
[15] Kumar A, Suman BM. Experimental evaluation of insulation materials for walls and roofs and their impact on indoor thermal comfort under composite climate. Build Environ 2013;59:635–43.
[16] Singh K, Muljadi BP, Raeini AQ, Jost C, Vandeginste V, Blunt MJ, et al. The architectural design of smart ventilation and drainage systems in termite nests. Sci Adv 2019;5(3).
[17] Ozel M. Thermal performance and optimum insulation thickness of building walls with different structure materials. Appl Therm Eng 2011;31(17–18):3854–63.
[18] Briga-Sa A, Nascimento D, Teixeira N, Pinto J, Caldeira F, Varum H, et al. Textile waste as an alternative thermal insulation building material solution. Construct Build Mater 2013;38:155–60.
[19] Morakinyo TE, Dahanayake KWDKC, Ng E, Chow CL. Temperature and cooling demand reduction by green-roof types in different climates and urban densities: a co-simulation parametric study. Energy Build 2017;145:226–37.
[20] Ahn BL, Kim JH, Jang CY, Leigh SB, Jeong H. Window retrofit strategy for energy saving in existing residences with different thermal characteristics and window sizes. Build Serv Eng Technol 2016;37(1):18–32.
[21] Sun L. Distribution of the temperature field in a pavement structure. Struct Behav Asphalt Pavem 2016.
[22] China - total primary energy consumption. Knoema; 2020.
[23] Stritih U, Tyagi VV, Stropnik R, Paksoy H, Haghighat F, Joybari MM. Integration of passive PCM technologies for net-zero energy buildings. Sustain Cities Soc 2018;41:286–95.
[24] Li SH, Sun GF, Zou KK, Zhang XS. Experimental research on the dynamic thermal performance of a novel triple-pane building window filled with PCM. Sustain Cities Soc 2016;27:15–22.
[25] Han YL, Taylor JE. Simulating the Inter-Building Effect on energy consumption from embedding phase change materials in building envelopes. Sustain Cities Soc 2016;27:287–95.
[26] Ahangari M, Maerefat M. An innovative PCM system for thermal comfort improvement and energy demand reduction in building under different climate conditions. Sustain Cities Soc 2019;44:120–9.
[27] Schossig P, Henning HM, Gschwander S, Haussmann T. Micro-encapsulated phase-change materials integrated into construction materials. Sol Energ Mat Sol C 2005;89(2–3):297–306.
[28] Ahmad M, Bontemps A, Sallee H, Quenard D. Thermal testing and numerical simulation of a prototype cell using light wallboards coupling vacuum isolation panels and phase change material. Energy Build 2006;38(6):673–81.
[29] Khudhair AM, Farid MM. A review on energy conservation in building applications with thermal storage by latent heat using phase change materials. Energy Convers Manag 2004;45(2):263–75.
[30] Li A, Xu X, Sun Y. A study on pipe-embedded wall integrated with ground source-coupled heat exchanger for enhanced building energy efficiency in diverse climate regions. Energy Build 2016;121:139–51.
[31] Shen C, Li X. Thermal performance of double skin façade with built-in pipes utilizing evaporative cooling water in cooling season. Sol Energy 2016;137:55–65.
[32] Yan T, Li J, Gao J, Xu X, Yu J. Model validation and application of the coupled system of pipe-encapsulated PCM wall and nocturnal sky radiator. Appl Therm Eng 2021;194:117057.
[33] Yan T, Xu X, Gao J, Luo Y, Yu J. Performance evaluation of a PCM-embedded wall integrated with a nocturnal sky radiator. Energy 2020;210:118412.
[34] Kishore RA, Bianchi MV, Booten C, Vidal J, Jackson R. Optimizing PCM-integrated walls for potential energy savings in US Buildings. Energy Build 2020;226:110355.
[35] Souayfane F, Fardoun F, Biwole P-H. Phase change materials (PCM) for cooling applications in buildings: a review. Energy Build 2016;129:396–431.
[36] Tang K, Dong K, Li J, Gordon MP, Reichertz FG, Kim H, et al. Temperature-adaptive radiative coating for all-season household thermal regulation. Science 2021;374(6574):1504–9.
[37] Wang S, Jiang T, Meng Y, Yang R, Tan G, Long Y. Scalable thermochromic smart windows with passive radiative cooling regulation. Science 2021;374(6574):1501–4.
[38] Li BW, Wang L, Casati G. Thermal diode: rectification of heat flux. Phys Rev Lett 2004;93(18).
[39] Wehmeyer G, Yabuki T, Monachon C, Wu JQ, Dames C. Thermal diodes, regulators, and switches: physical mechanisms and potential applications. Appl Phys Rev 2017;4(4).
[40] Tso CY, Chao CYH. Solid-state thermal diode with shape memory alloys. Int J Heat Mass Tran 2016;93:605–11.
[41] Ghanekar A, Ji J, Zheng Y. High-rectification near-field thermal diode using phase change periodic nanostructure. Appl Phys Lett 2016;109(12).
[42] Martinez-Perez MJ, Fornieri A, Giazotto F. Rectification of electronic heat current by a hybrid thermal diode. Nat Nanotechnol 2015;10(4):303–7.
[43] Zhang T, Luo TF. Giant thermal rectification from polyethylene nanofiber thermal diodes. Small 2015;11(36):4657–65.
[44] Zhou Y, Cai Y, Hu X, Long Y. VO 2/hydrogel hybrid nanothermochromic material with ultra-high solar modulation and luminous transmission. J Mater Chem 2015;3(3):1121–6.
[45] Zhou Y, Cai Y, Hu X, Long Y. Temperature-responsive hydrogel with ultra-large solar modulation and high luminous transmission for "smart window" applications. J Mater Chem 2014;2(33):13550–5.
[46] Zhao L, Bhatia B, Yang S, Strobach E, Weinstein LA, Cooper TA, et al. Harnessing heat beyond 200 degrees C from unconcentrated sunlight with nonevacuated transparent aerogels. ACS Nano 2019;13(7):7508–16.
[47] Zhang Z-Y, Zhang C-L, Ge M-C, Yu Y. A frost-free dedicated outdoor air system with exhaust air heat recovery. Appl Therm Eng 2018;128:1041–50.
[48] Mumma SA. Designing dedicated outdoor air systems. ASHRAE J 2001;43(5):28–32.
[49] Berardi U, Soudian S. Experimental investigation of latent heat thermal energy storage using PCMs with different melting temperatures for building retrofit. Energy Build 2019;185:180–95.
[50] Khalifa AJN, Marshall RH. Validation of heat-transfer coefficients on interior building surfaces using a real-sized indoor test cell. Int J Heat Mass Tran 1990;33(10):2219–36.